It is surmised that because of the generally similar character of supersonic blunt-body pressure distributions these results will also be valid for other probe shapes and Mach numbers, provided the area of the hole is a reasonable fraction of the total frontal area, and, further, that it is symmetrically placed as probe II rather than probe I

Reference

[1] Gracey, W , Coletti, D E , and Russell, W R , "Wind tunnel investigation of a number of total-pressure tubes at high angles of attack," NACA TN 2261 (January 1951)

Chemical Scavenger Probes in Nonequilibrium Gasdynamics

D E Rosner,* A Fontijn,† and S C Kurzius†
AeroChem Research Laboratories, Princeton, N J

DIRECT, local measurements of atom, free radical, excited molecule, and/or ion concentrations are required in the experimental study of nonequilibrium flow fields and for calibrating high enthalpy test facilities In attempts to simulate the conditions of hypervelocity flight it is necessary to know whether the test gas composition (e g , population of excited states) is not, in some sense, singular, particularly when an electrical discharge is used to heat the gas Although gas-sampling techniques have been successfully applied to the study of local stable species concentrations both in subsonic and supersonic steady flows,[1–3] rapid heterogeneous and homogeneous reactions in the sampling system have precluded their direct use for unstable species We wish to point out here that this difficulty can frequently be eliminated by introducing a "scavenger" gas immediately inside the probe The scavenger rapidly and quantitatively reacts with the unstable species in the sampled gas to form one or more stable products, which can then be analyzed downstream by any one of a number of conventional techniques The authors have successfully applied this principle in sampling nonequilibrium supersonic streams of active nitrogen for both atoms and excited molecules Details of the experimental technique, and the implications of this work to our understanding of the chemistry of active nitrogen will be found in a forthcoming paper [4] Here we confine our attention to some of the implications for aerodynamic testing

The measurement of local excited molecule concentrations is made possible by the existence of scavengers that are selectively attacked by atoms and/or excited molecules Thus, nitrogen sampled from a Mach 3 plasmajet was reacted with nitric oxide, ammonia, or ethylene, and measurements were made of scavenger gas destruction (NO, NH_3), a gas-phase chemiluminescence titration end point (NO), and product formation (HCN from C_2H_4) An interesting conclusion of this work is that electronically excited nitrogen molecules can be present in concentrations comparable to that of ground-state atoms, and can thereby exceed the importance of atoms as energy carriers in nonequilibrium plasmajets Absolute atom and excited molecule concentrations determined using scavenger-probe techniques can now be used in conjunction with catalytic detector measurements[5 6] made under identical experimental conditions to determine the contribution of individual energetic species to gas/solid energy transport

Scavenger probes lend themselves to use in high-temperature systems since they can be (water) cooled and/or the scavenger gas can be mixed with an inert diluent The technique is generally useful for quantitative studies of the energetic species of interest in aerodynamic and chemical propulsion applications and may also be used to distinguish between various excited states of the same molecule It is relevant to point out that Fristrom has recently reported on an independent application of the scavenger-probe concept in subsonic, low-pressure flame studies [7 8] Oxygen atom, hydrogen atom, and methyl radical concentrations have been determined using, respectively, NO_2, chlorinated diffusion pump oil vapor, and iodine as the scavenging gases

Although a considerable amount of research has yet to be done, particularly with regard to analyzing mixtures of energetic species in supersonic streams, we feel that scavenger probes are destined to play an important role in the future of nonequilibrium flow diagnostics

References

[1] Tiné, G , *Gas Sampling and Chemical Analysis in Combustion Processes* (Pergamon Press, London, 1961), Sec B

[2] Fristrom, R M , "Experimental determination of local concentrations in flames," *Experimental Methods in Combustion Research-A Manual*, edited by J Surugue (Pergamon Press, London, 1961), Sec 1 4, pp 6–31

[3] Hottel, H C and Williams, G C , "Experimental techniques," *Design and Performance of Gas Turbine Power Plants* (Princeton University Press, Princeton, N J , 1960), Vol XI, Part 2, Sec C, pp 44–91

[4] Fontijn, A , Rosner, D E , and Kurzius, S C , "Chemical scavenger probe studies of atom and excited molecule reactivity in active nitrogen from a supersonic stream " AeroChem TP-47a (December 1963); also Can J Chem (submitted for publication); also presented in part before the Division of Physical Chemistry of the American Chemical Society, 142nd National Meeting, Atlantic City, N J , abstract, p 51T (September 9–14, 1962); cf AeroChem TP-40, ASTIA AD 296 398 (August 1962)

[5] Rosner, D E , "Diffusion and chemical surface catalysis in a low temperature plasmajet–the determination of atom concentrations in nonequilibrium supersonic streams of activated nitrogen, J Heat Transfer **C84**, 386–394 (November 1962)

[6] Rosner D E , "Catalytic probes for the determination of atom concentrations in high speed gas streams," ARS J **32**, 1065–1073 (1962)

[7] Fristrom, R M , "Scavenger probe sampling: a method for studying gaseous free radicals," Science **140**, 297–300 (April 1963)

[8] Fristrom, R M , "Radical concentrations and reactions in a methane-oxygen flame," *Ninth Symposium (International) on Combustion* (Academic Press Inc , New York, 1963), pp 560–575

Received July 17, 1963; revision received September 25 1963 Based on research supported by the U S Air Force Office of Scientific Research, Propulsion Division, under Contract AF 49(638)300

* Aeronautical Research Scientist Member AIAA
† Physical Chemist

Temperature Distributions Downstream of a Moving Heat Sink

Ashley F Emery*
University of Washington, Seattle, Wash

Nomenclature

a = half-width of the heat sink, ft
h = heat transfer coefficient, Btu/hr-°F-ft²
k = thermal conductivity of the plate, Btu/hr-°F ft
l = thickness of the plate, ft

Received September 13, 1963; revision received February 10, 1964

* Assistant Professor of Mechanical Engineering

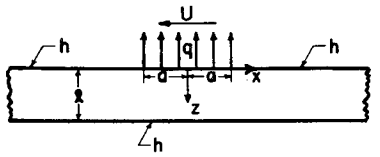

Fig 1 Plate cross section

q = strength of the heat sink, Btu/hr-ft²
x = distance along the plate, ft
T = temperature, °F
T_∞ = ambient temperature, °F
z = distance through the plate, ft
U = velocity of the heat sink, fps
κ = thermal diffusivity, ft²/sec

WHEN a small spill of a cryogenic liquid falls upon a metal plate and flows along its surface, large thermal stresses and deflections may be produced This is particularly so if the thickness is very small, as is commonly found in flight structures For a given plate, the magnitudes of these stresses and deflections are functions of the speed with which the packet of fluid moves along the surface The maximum deflection of the plate is proportional to the maximum induced bending stress and to the extent of the stressed region (i e , the length of the plate for which the temperature distribution is nonsymmetrical)

Consider the plate cross section shown in Fig 1 where the fluid packet is considered to be a sink of heat The plate is taken to be infinite in extent in the x and y directions and of thickness l in the z direction The heat sink, of width $2a$, travels from right to left with a uniform velocity U The heat-transfer coefficients on the upper and lower surfaces (outside of the sink region) are constant and equal to h The length of the stressed region is a maximum when the temperature is fully established

The steady-state temperature distribution in the plate may be obtained by suitable manipulation of Eq (17) of Ref 1 and is given by

$$T - T_\infty = \frac{-ql}{k} \sum_{n=1}^{\infty} \frac{(\beta_n^2 \cos\beta_n\bar{z} + \beta_n\bar{h} \sin\beta_n\bar{z})}{(\beta_n^2 + \bar{h}^2 + 2\bar{h})} \frac{K}{P_n} \Phi_n$$

where

$$\Phi_n = \frac{2K}{1+P_n} \exp\left\{\frac{1+P_n}{K}\bar{x}\right\} \sinh\left\{\frac{1+P_n}{K}\bar{a}\right\} \qquad \bar{x} < -\bar{a}$$

$$= \frac{+K}{1-P_n} \exp\left\{\frac{1-P_n}{K}(\bar{x}+\bar{a})\right\} - \frac{K}{1+P_n} \exp\left\{\frac{1+P_n}{K}(\bar{x}-\bar{a})\right\} + \frac{2P_n}{K\beta_n^2} \qquad -\bar{a} < \bar{x} < \bar{a}$$

$$= \frac{2K}{1-P_n} \exp\left\{\frac{1-P_n}{K}\bar{x}\right\} \sinh\left\{\frac{1-P_n}{K}\bar{a}\right\} \qquad \bar{x} > \bar{a}$$

and where

$$K = 2\kappa/Ul \qquad \bar{x} = x/l \qquad \bar{z} = z/l$$
$$\bar{a} = a/l \qquad \bar{h} = hl/k \qquad P_n = (1 + K^2\beta_n^2)^{1/2}$$

and β_n are the roots of $\tan\beta_n = 2\beta_n\bar{h}/(\beta_n^2 - \bar{h}^2)$ For values of hl/k ($= \bar{h}$,) less than 0 4, the roots are given approximately by $\beta_1 = (2\bar{h})^{1/2}$ to within 3%, and $\beta_n = (n-1)\pi$ for $n > 2$ to within 0 5%

The calculation of the temperature in the region near the heat sink ($\bar{x} \sim \bar{a}$) requires the evaluation of approximately the first 100 terms However, as we move away from the sink, the number of terms diminishes greatly as the variation of the temperature through the depth decreases An examination of the terms shows that, as long as $\cos\beta_n\bar{z}$ is approximately one, the terms are of the order $1/\beta_n^2$ If $\cos\beta_n\bar{z}$

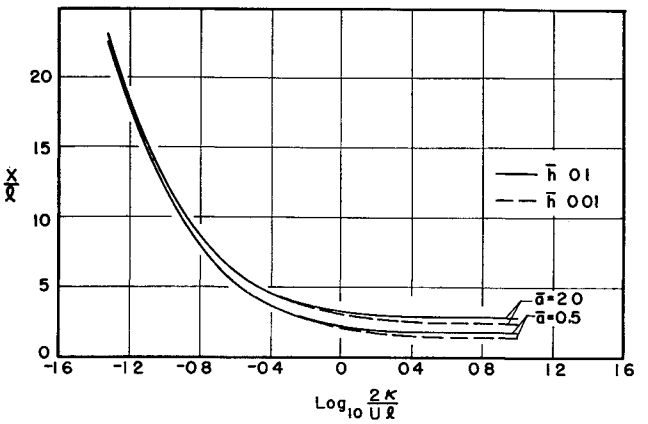

Fig 2 Values of $\bar{x}$ for which the temperature distribution in z is symmetrical within 1%

~ 0, then the terms are of order $\bar{h}/\beta_n^3$ The most critical situation will occur at $\bar{z} = 0$ For practical purposes, $h_{max} \sim 50$ (when exposed to moving air), $l \sim \frac{1}{24}$ ft, $k_{min} \sim 10$; thus $\bar{h}_{max} \sim \frac{1}{5}$ and $\beta_1 \sim (0\,4)^{1/2} \sim 0\,6$ Since $\beta_2 \sim \pi$, the ratio of the first two coefficients of the exponential terms for $\bar{x} > \bar{a}$ will be approximately 10:1 As soon as we move downstream of the sink region, the exponentials, which are of the form $\exp\{(-K\beta_n^2/2)\bar{x}\}$ for very small K (i e , thick plates or high velocity U) or of the form $\exp\{-\beta_n\bar{x}\}$ for large K, increase the ratio quickly, and as a result the temperature is essentially given by the first term of the series with small corrections added by the remaining terms Since, in general, $\bar{h} \sim 0\,2$ or less, the variation of the first term with $\bar{z}$ is only from $1/\beta_1^2$ to about $0\,9/\beta_1^2$, and the temperature will be approximately constant throughout the depth Obviously, as $\bar{x}$ increases sufficiently, at some value of $\bar{x}$ ($= \bar{x}_{c\ it}$) the thermal bending stresses vanish, since the temperature will have become symmetrical about $\bar{z} = \frac{1}{2}$ If one chooses the point $\bar{x}_{\ it}$ to be where the temperature distribution is symmetrical to within 1%, the following values of $\bar{x}_{\ it}$ vs K (Fig 2) for $\bar{a} = 0\,5$ and 2 are obtained For $K < 10$, the extent of the stressed region may be taken as $\bar{x}_{c\ it} + \bar{a}$, since there is no penetration of the temperature nonuniformity into the plate ahead of the moving fluid One can see that, even for the very high velocities, only a few thicknesses are necessary to establish the symmetrical temperature distribution For values of $K < \frac{1}{40}$, $\bar{x}_{\ it}$ is given by the relation $\bar{x}_{c\ it} \sim 1\ 1/K = 0\ 55\ Ul/\kappa$ The curves for different $\bar{h}$ coalesce because as U increases the amount of heat lost by the plate decreases, and the temperature variations are mitigated A numerical evaluation of the bending stresses for a fixed geometry shows that they are relatively independent of U, and consequently the maximum plate deflection is proportional only to $\bar{x}_{crit}$

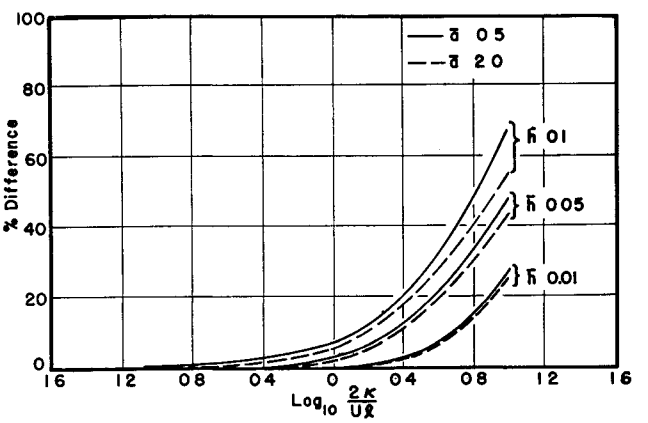

Fig 3 Difference between the exact and the extended fin solution at $\bar{x} = \bar{x}_{\ it}$

As a matter of interest in calculating the axial stresses, if the temperatures at $\bar{x} = \bar{x}_{c\ it}$ are calculated by using the simple fin solution

$$T - T_\infty = -\frac{ql}{k}\frac{2\bar{a}}{1/K + [(1/K^2) + 2\bar{h}]^{1/2}} \times \exp\left\{\left[\frac{1}{K} - \left(\frac{1}{K^2} + 2\bar{h}\right)^{1/2}\right]\bar{x}\right\}$$

some error will arise due to heat transfer by convection in the region $-\infty < \bar{x} < \bar{x}_{\ it}$ Figure 3 shows the error incurred

Reference

[1] Carslaw, H S and Jaeger, J C, *Conduction of Heat in Solids* (Oxford University Press, London, 1959), p 373

Drop Size from a Liquid Jet in a Longitudinal Electric Field

RICHARD L PESKIN* AND ROLAND J RACO†
Rutgers University, New Brunswick, N J

A relationship between the drop sizes found by the breakage of an unstable liquid jet with and without the presence of a longitudinal electric field is developed Experimental results are in satisfactory agreement with the relation derived

Introduction

EXCEPT for the classic example of a liquid issuing from a nozzle to form a jet, investigations of the dynamic stability of jets have not given much information on the resulting drop size found when the jet breaks up because of instability In the classic example, as Plateau[1] first showed, the cause of instability is the surface tension which makes the cylindrical jet an unstable figure of equilibrium In this case, Rayleigh[2] finds that the most probable drop diameter d (i e the drop diameter formed at the mode of maximum instability) for a jet of radius R is given by $d = 4\ 508R$ However, little information is given on the resulting drop size for other cases of instability which include the presence of an electric field,[3,4] a magnetic field,[5,6] any motion of the jet,[5] or a surrounding fluid [5,7] The purpose of this paper is to study analytically and experimentally the size of the drops formed from an unstable jet when a longitudinal electric field is present

Analytical Study

Since for all cases of instability the most probable drop size is formed at the mode of maximum instability, one begins by first finding the mode of maximum instability Generally, it is found by perturbation of the Lagrange differential equation for the amplitude a of the deformation of the jet The resulting perturbation equation, which gives the criterion for stability, is then maximized to give the mode of maximum instability

In the classic case of the liquid jet, by assuming $a = \text{const} \times e^{\pm pt}$, the perturbation equation obtained is

$$p^2 = [xI_0'(x)T/I_0(x)\rho R^3](x^2 - 1) \qquad (1)$$

Received January 27, 1964 This work has been supported by the American Petroleum Institute

* Associate Professor, Department of Mechanical Engineering
† Research Assistant, Department of Mechanical Engineering

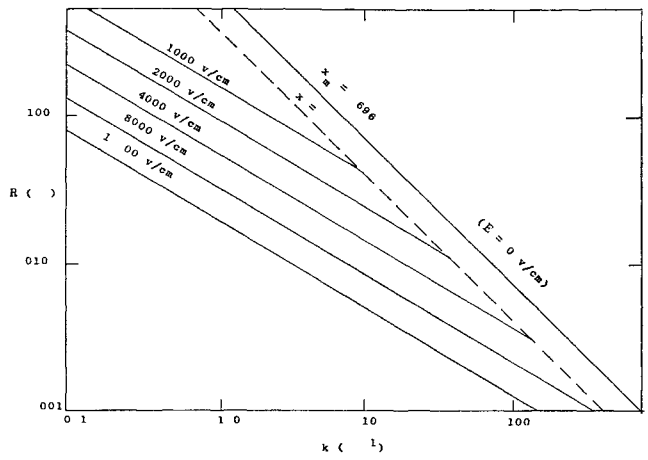

Fig 1 Relation between jet radius and wave number

Here R is the radius of the jet, T is the surface tension of the jet, ρ is the density of the jet, $x = Rk$, where k is the wave number, and I_0 is the zero-order Bessel function of the first kind for a pure imaginary argument The value x_m that causes p to be a maximum is given by Lamb[2] as $x_m = 0\ 696$ The plot of

$$x_m = kR = 0\ 696 \qquad (2)$$

for R vs k is shown in Fig 1

Following the foregoing procedure for the case of a jet in a longitudinal electric field **E**, Nayyar and Murty[4] obtain

$$p^2 = \frac{xI_1(x)}{\pi\rho R^2 I_0(x)} \times \left\{\frac{\pi T(1 - x^2)}{R} - \frac{(\epsilon_2 - \epsilon_1)^2 E^2 x I_0(x) K_0(x)}{4[\epsilon_1 I_1(x) K_0(x) + \epsilon_2 I_0(x) K_1(x)]}\right\} \qquad (3)$$

for the perturbation equation Here ϵ_1 is the dielectric constant of the jet, ϵ_2 is the dielectric constant of air, and K_n is the nth-order Bessel function of the second kind for an imaginary argument To find x_m, one considers $x \ll 1$ so that the Bessel functions can be replaced by their dominant terms One finds

$$x_m^2\left[-\gamma - \frac{1}{4} - \ln\frac{x_m}{2}\right] = \frac{2\pi\epsilon_2 T}{(\epsilon_2 - \epsilon_1)^2 E^2 R} \qquad (4)$$

Here γ is Euler's const = 0 577 For a jet issuing into

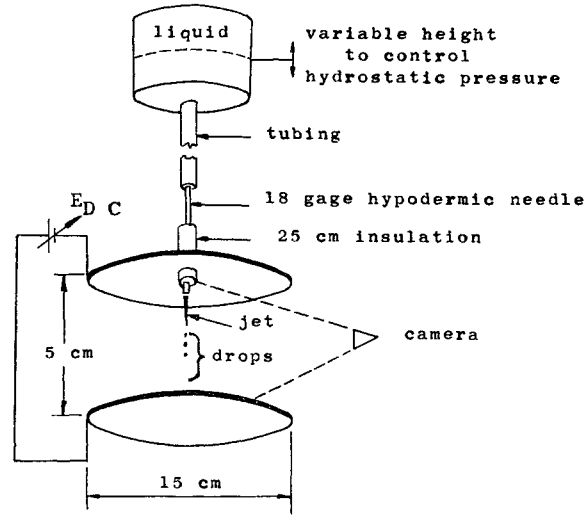

Fig 2 Experimental apparatus for producing and measuring d_i/d_E